Modeling the Spatial and Luminosity Distributions of X-Ray Binaries: An Introduction to the StarChart Code

Tim Linden

Supervisor: Prof. Vicky Kalogera

May 8, 2008

1. Introduction

X-Ray Binaries (XRBs) are two body systems consisting of a compact object, such as a neutron star or black hole, in tight orbit around a nuclear-burning star. Mass from the nuclear burning star is transported into the deep potential well of the compact object, gaining substantial kinetic energy which is then radiated with a characteristic X-Ray spectrum. There are two mechanisms capable of transporting stellar material from a nuclear burning star onto a compact object. In the closest binaries, the first Lagrange point may reside inside the envelope of the nuclear burning star. Matter spilling over the Lagrange point will fall onto the compact object. For slightly wider systems, bright X-Ray accretion can still result when some matter emitted in the stellar winds of the donor subsequently falls onto the compact object.

Through the careful study of pulsars, it has long been known that systems containing compact objects possess much larger proper velocities than systems containing probable compact object progenitors (Gunn & Ostriker 1970). This is not surprising, given the extreme violence of supernova explosions. Due to the complexity of supernovae, the exact reason for their non-isotropy is not yet certain, and thus all current stellar models impart compact objects with velocities corresponding to observational data. Many distributions of supernova "natal" kicks have been suggested, with significant disagreement over both the mean kick velocity and the number of relevant kick distributions. Cordes & Chernoff (1998) studied the positions of pulsars assuming each to have formed somewhere in the galactic plane and using spindown data to determine the age of each system. They found the distribution of kicks to be best fit by a two component Gaussian with means 175^{+19}_{-24} and 700^{+300}_{-132} km s^{-1} containing $\sim 86\%$ and $\sim 14\%$ of systems respectively. Hobbs et al. (2005) instead acquired proper motion data on 233 pulsars from a variety of sources, and proposed the data to be fit by a single Maxwellian distribution with mean 265 km s^{-1}.

Black holes are assumed to undergo natal kicks through the same mechanism as

neutron stars. However, observational detection of black hole proper velocities is extremely difficult. It is commonly assumed that black hole kicks are smaller than neutron star kicks by a factor relating to the amount of matter which began to escape from the black hole in the supernova explosion, but subsequently fell back onto the black hole, known as the fallback mass (Belczynski et al. 2008). The exceptions to this phenomena are extremely massive black holes which are thought to be formed via direct collapse, with all matter falling back onto the black hole. These systems are assumed to have zero natal kick (Fryer & Kalogera 2001).

As XRBs are among the brightest point objects in the galaxy, they form an important tool in extragalactic astronomy. Because all bright XRBs must contain a neutron star or black hole, the existence of an XRB is correlated with recent star formation in its stellar neighborhood (Grimm et al. 2003). Because of this, it has been speculated that they should be highly associated with large regions of intense star formation known as super star clusters (SSCs) (Fabbiano 1989; Makishima et al. 2000). SSCs are young, ultraluminous, and due to their extreme density, are thought to be self-gravitating and dynamically important for stars formed throughout the region. Due to their similarities with other dynamically important galactic structures, much speculation has been raised as to whether they are the young progenitors of galactic clusters (Ho & Filippenko 1996).

There are several nearby galaxies which exhibit signs of massive star formation localized to numerous SSCs surrounding the galactic core. These galaxies, called "starbursts", are detected due to the bluer than expected spectral lines which correspond to a multitude of newly formed massive stars. While much remains unknown about the mechanism of starburst activity, they are thought to be triggered by the merger of the galactic core with gas clouds capable of rejuvenating the galaxy (Gonzalez-Delgado et al. 1995; Barnes & Hernquist 1991). Due to the high formation rate of stars large enough to undergo supernova events, starburst galaxies are a prime location for evaluating the processes of

XRB formation. One particular starburst, NGC 1569, acted as an impetus to our work, both because of its recent star formation episode, and the existence of a well established dataset of its SSC and XRB population.

1.1. NGC 1569

NGC 1569 is a dwarf galaxy located $\sim$2.2 $\pm$ 0.6 Mpc from the Milky Way with a total stellar mass of $\sim$3.3 x 10^8 M$_\odot$ (Israel 1988). The northern half of the galaxy underwent a recent burst of star formation over the last 20 Myr (Hunter et al. 1982; Israel & de Bruyn 1988; Waller 1991). Stil & Israel (1998) find this outbreak to conincide with the passage of a 7 x 10^6 M$_\odot$ HI cloud approximately 5 kpc from the galactic center.

Two SSCs, aptly named "A" and "B", were discovered by Arp & Sandage (1985). Due to the massive size and young age of these clusters, multiple studies have attempted to determine their specific properties. Cluster "A" was found to contain both old red supergiant and young Wolf-Rayet stars, signaling the presence of two distinct stellar populations (Gonzalez Delgado et al. 1997). However, de Marchi et al. (1997) used WFPC2 observations to resolve this problem, determining Cluster "A" to actually be composed of two nearby clusters, with slightly different ages.

In addition to these two massive SSCs, recent observations have found myriad smaller clusters which form a background throughout the central region of NGC 1569. Hunter et al. (2000) found a population of 48 resolvable SSCs, providing half light radii and luminosities at three different wavelengths. Anders et al. (2004) (hereafter A04) provided an exhaustive list of 169 clusters, determining the most likely ages, masses, metallicities, and half light radii of each. Their results show that the more massive clusters preferentially formed early on in the starburst period. However, there are only 17 clusters jointly identified by each group, a discrepancy stemming primarily from the larger sampling field of Hunter et al.

4

(2000), and A04's rejection of small clusters in close proximity to much larger cluster.

The dynamic structure of NGC 1569 has also been heavily studied. Recchi et al. (2006) used hydrodynamical simulations to model the evolution of NGC 1569, matching models with known chemical abundances. To model the rotating gases, they introduce a two source galactic potential consisting of a dark matter halo with a core raidus of 1 kpc. The distribution is truncated at 20 kpc in order to keep the total mass finite. They set the total mass of this halo to be 1.4×10^9 M$_\odot$, but note this value is poorly constrained, with Reakes (1980) finding a value of approximately 5.0×10^8 M$_\odot$. The luminous matter in NGC 1569 provides the second contribution to the galaxy dynamics. Finally, in order to match the results of Reakes (1980), which found an approximately 1 to 2 ratio between the minor and major axis, they followed methods previously employed in (Recchi et al. 2001) to create a mass distribution following a stellar King profile of the form

$$\rho_*(R, z) = \rho_{*0}[1 + (\frac{R}{R_{c*}})^2 + (\frac{Z}{Z_{c*}})^2]^{-\frac{3}{2}} \tag{1}$$

For NGC 1569 they used $R_{c*} = 192$ pc and $Z_{c*} = 96$ pc along with trucation radii of $R = 960$ pc and $Z = 480$ pc in order to obtain a finite mass, setting ρ_{*0} in order to recover the total stellar mass of the galaxy obtained by Israel (1988) (Simone Recchi, 2007, private communication).

2. Motivation

With the launch of the *Chandra* X-Ray Observatory in 1999, it became possible to accurately track the position of X-Ray sources with sub-miliarcsecond precision and separate point sources from background galactic X-Rays. The wealth of discovered X-Ray point sources has allowed for detailed analysis and categorization of these objects. Of these systems, we determined NGC 1569 to lend the best opportunity for model formation as it has the most complete dataset available for SSC and XRB properties.

Martin et al. (2002) used spectral imaging from *Chandra* observations in order to detail the X-Ray content of NGC 1569. They find 45 bright X-Ray point sources above a cutoff luminosity of approximately 1 x 10^{36} erg s^{-1}, twelve of which were determined to be XRBs. The rest of these sources are attributed mainly to foreground stars or background active galactic nuclei. They provide position and luminosity data for each source, noting that no XRBs are found coincident with either Cluster "A" or "B".

Using the Martin et al. (2002) dataset, among others, Kaaret et al. (2004) (hereafter K04) studied three starburst galaxies, M82, NGC 1569 and NGC 5253, using *Chandra* observations to compare the position of X-Ray point sources against SSCs previously discovered in each galaxy. They found X-Ray point sources to be preferentially located near large star formation regions. However, there was a significant lack of sources found coincident with the SSCs themselves. They found this result to support the conclusion that many of these bright X-Ray sources are in fact XRBs which were removed from the cluster due to natal kicks imparted to the compact object in each system. Furthermore they find a gradient in source luminosity, with the brightest sources being restricted from moving far from the cluster center. They infer from this distribution that strong natal kicks inhibit the formation of bright binary systems.

There is however, an important limitation on observational analyses of XRB and cluster positions. Almost no velocity data is currently available on extragalactic XRBs. Thus there is method by which observations can determine where a given XRB was formed. This is an unfortunate limitation, as obtaining information about the populations of XRBs produced in each SSCs would provide an extremely useful bank of information from which to learn about the formation and evolution of massive stars. Here we undertake simulations designed to determine the current theoretical predictions for XRB formation from each SSC in NGC 1569, in order to compare the pathways for XRB production in each cluster, and determine which cluster XRBs are most likely to be formed in.

2.1. Prior Efforts

Sepinsky et al. (2005) (hereafter S05) first created the *StarChart* code in order to quantify the impacts of natal kicks on the observed positions of very young XRBs compared to parent SSCs. Using the *StarTrack* population synthesis code developed by Chris Belczynski (Belczynski et al. 2005, 2008), S05 simulated a population of bright XRBs formed free from any outside disturbance in a delta function star formation event. Obtaining a dataset containing the luminosities and natal kick velocities of all bright XRBs at densely populated time steps, they placed the XRB progenitors into cluster potential wells of various strengths and recorded their position as a function of time. Using the prescription of Plummer (1911), they employed a potential of form:

$$\Phi = -\frac{GMm}{\sqrt{r^2 + b^2}} \tag{2}$$

where b is related to the half mass radius of the cluster by a constant of order unity. Following the prescriptions of Aarseth et al. (1974), S05 then generated random initial positions such that the mass distribution of points creates the desired potential. Following the same prescription, they generate initial velocities such that the virial theorem is satisfied and the cluster does not collapse or fly apart over time.

S05 tested a range of several cluster masses, initial mass functions (IMF) and half mass radii. The number and distribution of bright XRBs were checked at ages of 10, 15, 20, 25, and 50 Myr after the star formation event and averaged over many runs of the same code. Employing bolometric calculations to compare modeled X-Ray emission with *Chandra* observations (best detailed in Belczynski et al. (2008)), they used a luminosity cutoff of $L_X = 5 \text{ x } 10^{35}$ erg s^{-1} in order to compare their results with several extragalactic sources, NGC 1569, NGC 5253, and M82.

S05 showed that a large population of XRBs are ejected from the potential wells of their parent SSC due to the supernova kick associated with compact object formation.

The ratio of ejected to bound XRBs was found to be significantly dependent on the age of the XRB population. At 10 Myr, the median distance between an XRB and parent cluster is between 9 and 13 pc for all simulations, while at 50 Myr, the median distance is approximately 100-150 pc. They attribute this relation to the decreased time between natal kick formation and observation of the bright XRB. S05 find the dependence on cluster mass and half mass radius to be significantly less, because XRB natal kicks are significantly more energetic than the gravitational potential of the largest SSCs. They also find the number of bright XRB sources to approximately match the number observed in several starburst galaxies, though they note that the many uncertainties in stellar population synthesis allow their results to match a wide variety of potential systems.

2.2. Opportunities for Improvement

Despite these advances, the S05 code is limited in several respects. Most importantly, their analysis is constrained to studying the gravitational effects of a single SSC in the absence of any galactic mass distribution. The significant mass of galactic cores can affect the spatial distribution of XRBs in several ways. First, an XRB that becomes unbound from it's parent cluster may not become unbound from the much larger galactic potential. Secondly, even unbound XRBs may be scattered off of the galactic potential, creating a non-isotropic XRB distribution.

Another restriction in the S05 code is the inability to compare the interactions of XRBs with a full population of SSCs. While K04 showed that XRBs are preferentially found near clusters, they did not show that XRBs are found near their parent cluster. An improved theoretical model would be able to show the number of XRBs which are only near an unrelated cluster, in order to determine whether K04 greatly overestimates the number of close XRBs. This requires a full galactic model including the spatial distribution of SSCs.

8

3. Code Description

In order to allow the modeling of a dynamic galaxy, a multitude of alterations to the *StarChart* code used in S05 were necessary. Our code now allows XRBs to be created for as many SSCs as the user chooses, and the number of XRBs formed around each cluster corresponds to the clusters mass. Since we have a clear hierarchy of masses ($\mathrm{M}_{XRB} \ll \mathrm{M}_{SSC} \ll \mathrm{M}_{Galaxy}$), we are able to ignore the impact of XRB-XRB and Cluster-Cluster interactions in order to avoid a full N-body calculation, as N would be on the order of hundreds of millions for any reasonable galactic model. Instead, we work from the reference frame of the galaxy, and evolve each individual XRB in a restricted three-body problem consisting of the galactic potential, the parent SSC, and the XRB itself. If desirable, the gravitational potential of all other clusters can be calculated as a background affecting the three-body system. At the end of the evolution period, we have spatial and luminosity information on all XRBs formed in our simulation of the galaxy. Since we know which SSC each XRB formed in, we are able to compare the distribution of XRBs with regard to both the parent and background SSCs.

The revised *StarChart* code is written to be integrated into the Portable Batch System (PBS), which is a job scheduling platform designed for use on multi-processor cluster environments. The code, however, does not directly take advantage of the parallel processing capabilities of Beowulf clusters, chiefly because it employs the existing *StarTrack* code, which is not designed for parallel computation. Instead, we capitalize on the approximation that each XRB is kept dynamically independent of all other XRBs and instruct our main bash script to read in data on all SSCs that the user has supplied, submitting a model corresponding to the XRBs formed in each cluster. These PBS scripts may then be distributed to each node or run concurrently on a single processor system.

StarChart contains four base modules, and is designed to allow end user flexibility with respect to the creation of analysis routines and input parameters. The four modules

are (in order of execution) Randomize, StarTrack, StarChart, and Analysis. Each module is controlled by a Bash script which executes all processes taking place in that module.

3.1. Randomize

The Randomize module runs on the main processor before PBS submission and controls all processes which must be synchronized between each cluster. Due to the almost complete independence of each cluster, this is a simplified alternative to implementing MPI and allowing true node-node communication. The randomization routine could easily be abridged to allow synchronous random number generation or synthesis of cluster and galactic potentials if the end user deems necessary. However, in the current implementation, it's only relevant role is to evolve each SSC backwards in time from its observed current position, to a possible position at the beginning of the simulation. This must be done before sending data to each node, as it is important for every node to have the same galaxy layout at the beginning of the simulation.

For a dwarf galaxy modeled by a Plummer potential with mass on the order of 10^9 M$_\odot$ and a half mass radius on the order of 1 kpc, an XRB in a circular orbit would be traveling at a rate of 84 pc Myr^{-1}. Since we intend this code to analyze starbursts which occurred between tens and hundreds of Myr ago, we cannot evolve the system from its presently recorded position and expect our results to match against observations. We also cannot assume that the entire simulation occurred in clusters static with respect to the galactic potential. This present two problems. First an XRB which received a natal kick 5 Myr before the end of the simulation would have been kicked away from a very different location than the present position of the cluster. Secondly, without a moving cluster, XRBs near the galactic potential would rarely be bound to the cluster potential, and almost all will begin orbiting the galactic potential. Unfortunately, current velocity data in general is not

available for extragalactic SSCs, and thus we are left to artificially create SSC velocities.

In order to confront this problem, we create random cluster velocities following the prescription in Aarseth et al. (1974). Using the time invariance of Newton's laws, we then evolve these systems backwards in time for the duration of the simulation, obtaining final velocities for our back evolution. Taking the opposite velocities, and noting the isotropy of the Plummer potential, we have now created a random initial velocity distribution in accordance with Aarseth et al. (1974). Furthermore, each set of initial positions and velocities is guaranteed to return the cluster to its observed location at the end of the simulation. Unfortunately, this velocity is completely random and may have no correlation with the actual velocity of the cluster. Even over the course of many runs, we will not converge on the correct result for a moving cluster, because our randomly generated isotropic velocities will tend to cancel each other out, whereas the cluster has a definite non-zero velocity. However, generating these results for many runs, we will at least be able to analyze the impact that different cluster velocities have on the resultant XRB distribution.

3.2. StarTrack

StarTrack, written by Chris Belczynski (Belczynski et al. 2005, 2008) is a population synthesis code designed to simulate star formation and evolution in accordance with myriad theoretical models and observational constraints. First, a random binary system is created from a large parameter space of stellar masses, binary separations, eccentricities and other variables. Then the systems are evolved analytically using derived equations of state. Because the existence of a binary companion has little influence on the evolution of most single stars, each star is evolved along the single star evolution tracks produced by Hurley et al. (2000). However, in close binaries, common envelopes, mass transfer, and magnetic

11

breaking are included, in order to create accurate binary systems.

The *StarTrack* code allows for enormous fine tuning of the population synthesis model, including myriad algorithms for wind mass loss, tidal effects, kick velocity distributions, common envelope, mass transfer efficiencies etc. A full explanation of these choices is beyond the scope of this work, so we refer to Belczynski et al. (2008) for a complete description of the *StarTrack* code. However, we must make note of several important concepts used in our analysis.

In order to run the StarTrack code, we must first create the *StarTrack* input file for each SSC the user is planning to simulate. Using an automated script, the user can quickly set many important variables including the initial mass function, binary fraction, minimum and the maximum primary and secondary masses used in the code. *StarChart* must also determine the number of XRBs to simulate in order to recreate the conditions in a SSC of a given mass. As in S05, we adopt an initial mass function, $f(m1)$, for the primary star, a mass ratio $0 < q \leq 1$ which determines the ratio of the secondary mass to the primary mass, and a binary fraction f_{bin}. Given total mass of a star formation region and a bound M_{min} on stellar masses, we want to find the total number of binaries with a minimum primary mass (M_{Xmin}) large enough to form a neutron star or black hole. We can calculate the number of XRB progenitors from the equations

$$M_{tot} = f_{bin} \int_{M_{min}}^{\infty} \int_{0}^{1} [f(m_1)m_1 + f(m_1)g(q)m_1q]dqdm + (1 - f_{bin}) \int_{M_{min}}^{\infty} f(m_1)m_1dm_1 \quad (3)$$

$$N_{bin}^{tot} = f_{bin} \int_{M_{Xmin}}^{\infty} f(m_1)dm_1 \quad (4)$$

where g(q) is the probability that a binary will have a mass range of q. For data presented in this paper we set the mass of the primary using the Salpeter distribution $f(m_1) \sim M^{-2.35}$, set g(q) to be a uniform distribution with $M_{min} = 0.15$ $M_{\odot}$. Because we are interested only in systems which are large enough to become XRBs, we set a minimum bound $M_{Xmin} = 4$ $M_{\odot}$ on the mass of the primary star in order to find the number of systems to

run in *StarTrack.*

3.3. StarChart

The StarChart module reformats *StarTrack* output data for *StarChart* input and then executes the *StarChart* code. There are two output files relevant to XRBs in *StarTrack*, DetWIND.dat and DetMT.dat, which display data for wind accretion and mass transfer XRBs respectively. Of course, a system can potentially alternate between wind accretion and mass transfer repeatedly during it's lifetime. Because *StarTrack* ouput files may contain many gigabytes worth of data, reading in both files and simultaneously accessing the information from each is not a reasonable option on most computers. Thus, in order for *StarChart* to evolve a single system, these files must be merged such that each binary system has a contiguous and chronologically ordered position in the input file.

In addition to a Plummer potential for our SSCs, we allow XRBs to respond to any number of static "galactic" potentials. As most galaxies are non-spherical, we employ the the Pummer-Kuzmin potential from Miyamoto & Nagai (1975)

$$\Phi(R, Z) = -\frac{GM}{\sqrt{R^2 + (a + \sqrt{Z^2 + b^2})^2}} \tag{5}$$

We note that in the case a=0, this reduces to a Plummer potential, while setting b=0 reproduces the flat-disk Kuzmin potential. While the code could be employed to allow a wider variety of potentials, galaxies obey none of the above, and even approximations of most galactic potentials are highly uncertain. Furthermore, as noted earlier, multiple Plummer-Kuzmin potentials can be employed to approximate any chosen potential.

Before XRB evolution commences we must evolve the clusters independently around the galactic potential. This is done for two reasons. First, since we evolved our SSCs backward in time in order to calculate the position of each cluster at time t=0 (the time

of the star formation event of the oldest cluster), we must find the position of the cluster at the time our XRBs were generated. Without this information we would be unable to begin the three-body evolution of each XRB at the correct position. Secondly, if the user has enabled the gravitational interaction of our three body system with the background potential, we must have a rough idea where the other clusters are at each point in time. Thus, an appropriately dense dataset of cluster positions is stored in an array, and the exact position of all clusters is interpolated from this dataset whenever a calculation requiring a cluster besides the parent cluster is needed.

We place each input XRB into our cluster potential at the time of the SSC star formation event, following the prescription of Aarseth et al. (1974). Because we want our XRBs to be uniformly distributed about the SSC, we ignore the galactic potential when assigning initial positions for the XRB. However, we must take into account the fact that the SSC has a non-zero velocity compared to the galaxy, and thus we calculate the initial XRB velocity by

$$\vec{v}_{XRB} = \vec{v}_A + \vec{v}_{SSC} \tag{6}$$

where $\vec{v}_A$ is the XRB velocity relative to the cluster determined by Aarseth et al. (1974) and $\vec{v}_{SSC}$ is the velocity of the SSC compared to the galaxy.

In order to evolve the system, we create a restricted three body problem by calculating the gravitational interaction between the galactic, cluster, and XRB potentials in the inertial frame of the galaxy. If the user has enabled interaction between this system and the other background SSCs, the gravitational force between these potentials and the SSC-XRB system is applied to the XRB-Cluster only, with the positions of other clusters computed via interpolation from the datapoints saved in the preliminary run. At the time of the supernova event of the primary star in each XRB progenitor, the binary receives a natal kick with a velocity recorded by *StarTrack*. When *StarChart* encounters a datapoint indicating a natal kick, the code adds the kick velocity onto the current XRB velocity

assuming an isotropic kick distribution. Upon completing the evolution of a given XRB, the position of the cluster is reset to its position at the time of the starburst event of the cluster. For all three body integrations, we use the ordinary differential equation integrator `odeint` from Numerical Recipes in order to quickly evolve the systems, outputting data with a user specified timestep.

As in S05, we apply bolometric corrections to the X-Ray luminosities of each binary in order to compare our results to *Chandra* observations. Following the procedure set forth in Belczynski et al. (2008), we multiply our calculated X-Ray luminosity by 0.7 for all black hole systems, 0.5 for mass transfer neutron stars, and 0.15 for neutron star wind accretion systems. The method of interpolating between *StarTrack* output luminosities has been substantially improved, the interpolation is now performed logarithmically in order to prevent overdetection of bright sources. Extrapolation from the first and last datapoints has also been disabled, as it was shown to overemphasize systems which should have zero luminosity according to an analysis of the *StarTrack* calculations.

Because each XRB is evolved based on only dynamic considerations, a simple diagnostic for the program is to calculate the total energy of the system at every timestep and look for violations of the conservation of energy. Except at the time of the supernova event of the primary star, the total energy should remain constant. However, we note that this is not true if the influence of other moving clusters are computed, both because the parent cluster does not pull back on these background SSCs, and because we lack a stationary reference frame from which to evaluate the energy.

There are several optimizations employed in the revised *StarChart* code not present in older versions. Most notably, the previously combined *StarTrack* output file is prescanned to determine which systems have the possibility of becoming bright near the point of analysis. If a system does not become bright near the time of the computation, the user has the option of rejecting analysis of the system, saving considerable time in the tracking of bright

systems. This option can be disabled if the tracking of non X-Ray bright sources is desired.

3.4. Analysis

The Analysis module contains all post-processing analysis routines and controls automatic data packaging and compression. This portion of the code is meant to be extremely customizable in order to create whatever datasets the end user wants. The current code analyzes all XRBs at the end of the simulation, determining the number and position of bright XRBs. Graphs detailing the number of XRBs within a given radius of the SSCs final position and the X-Ray luminosity function of each cluster are created.

4. Modeling of NGC 1569

In Table 1 we show adopted properties that we believe to closely mirror NGC 1569. In order to recreate the dynamic environment of the starburst regions in NGC 1569, we create a two component galactic potential using the specifications for a 1.6 x 10^9 M$_\odot$ dark matter halo in addition to a 3.3 x 10^8 M$_\odot$ Plummer-Kuzmin potential with a=50 and b=240 in order to recreate the oblate King sphere potential used by Recchi et al. (2006). While our stellar potential does not exactly replicate a King sphere potential, we note that only the mass and two to one ratio of the axes is specified by observational evidence. Thus, while we attempt to closely fit the Recchi et al. (2006) model, there is no observational reason to prefer one model over the other.

We adopt the A04 dataset of NGC 1569 SSCs in order to position our clusters around the galactic potential. However, we find that many of the clusters are so small as to make their XRB contribution negligible. We thus set a cutoff mass of 5 x 10^4 M$_\odot$ for SSCs, which restricts the A04 dataset to 13 clusters which contribute the vast majority of star

formation in NGC 1569. We note K04 preferentially found XRBs near these larger SSCs. In accordance with the A04 dataset, we do not consider Cluster A as a double cluster, since A04 find both the cluster ages and the amount of matter separated into each cluster to be highly uncertain. While there are sometimes significant uncertainties in the A04 observations of mass, age, and metallicity, we do not consider variations in these values as this is merely a test of the feasibility of our models. However, we will consider variations in our initial parameters in Section 5

There are many significant obstacles in creating three-dimensional dynamic models from two-dimensional luminosity based observations. All masses and half mass radii must be generated using luminosity-mass relationships. While A04 has already employed this method to determine cluster masses, we adopt a 1:1 correspondence between the half-light and half mass ratio (de Grijs et al. 2002). Velocity data for extragalactic objects is unavailable, as is any measurement of the relative depth of SSCs or XRBs along the line of sight. NGC 1569 is tilted 60 degrees from edge on, thus all XRB and cluster positions are projected accross this line of site. Without a measurement of depth we place SSCs directly on the galactic plane. In the case of NGC 1569, there is no measurement of the dynamical center of the galaxy. Here we adopt a measurement of the luminous center of the galaxy produced by Waller (1991).

In order to model the NGC 1569 star formation rate, we must adopt many theoretical parameters. Setting t=0 as the creation time of the oldest cluster (A04's Cluster 35, which, at 8.86 Gyr old, is a large galactic cluster), we then set t=8860 Myr as the present. Each cluster undergoes a delta function star formation event following a Salpeter ($M^{-2.35}$) initial mass function at the the time at which the cluster was formed, in accordance with A04 observations. We set the minimum progenitor masses above 4 $M_\odot$ for the primary and 0.15 $M_\odot$ for the secondary in order to evaluate both all high mass and low mass XRBs. Supernova kicks are computed using a single Maxwellian kick distribution with mean

265 km s^{-1} (Hobbs et al. 2005). We assume conservative mass transfer. Finally, in order to obtain statistically significant results, we run 50 simulations of the clusters and average the final results.

5. Results

Our analysis has produced several useful results. One unfortunate finding is that our XRB population is dominated by Cluster A, which makes analysis of the interplay between the clusters somewhat less interesting. In Figures 1 through 3 we use a cumulative distribution function to show the distance of bright XRBs from both their parent cluster and the nearest cluster (including the parent) for Clusters A, B, and A04's Cluster 143 (Cluster 35 in Hunter et al. (2000)). We find that these three clusters produce the most XRBs and also have similar properties that allow us to isolate individual variables which affect XRB production. In Table 2 we note important information for these three clusters.

Immediately we note very different results for our three SSCs. Cluster A displays a two peak distribution. Approximately 30% of all bright XRBs remained within 10 pc of the SSC. We note that there are almost no XRBs between 10-100 pc from the Cluster. Approximately 70% of all XRBs have travelled over 100 pc from Cluster A. In Cluster B, the situation is different, approximately 50% of XRBs have stayed within 10 pc of the cluster center, with 50% of systems greater than 60 pc from the cluster. On the contrary, in Cluster 143, almost all XRBs are farther than 1000 pc from the SSC. Observationally, we note that many XRBs farther than 1 kpc from the studied SSC center would not be detected as they outside the range examined by observers.

In Figures 4 through 6 we depict the luminosity and distance from the parent cluster for every XRB formed by the three model clusters. We find three distinct populations of XRBs: close and high luminosity XRBs, often with luminosities $\sim 10^{39}$ erg s^{-1}, close and

Table 1: Adopted Properties of NGC 1569

Property	Value
R.A.$(1950)^a$	$04^h26^m05^s$
Decl. $(1950)^a$	$64°44'24"$
Distance^b	2.2 Mpc
Black Matter Halo Mass^c	$1.9 \times 10^9 M_\odot$
Stellar Mass^b	$3.3 \times 10^8 M_\odot$

[a] Waller (1991)

[b] Israel (1988)

[c] Recchi et al. (2006)

Table 2: Important NGC 1569 Clusters

Cluster Name	Mass ($M_\odot$)	Age (Myr)	Metallicity	Half Mass Radius (pc)
Cluster A	1.64 x 10^6	12	0.0004	2.69
Cluster B	5.65 x 10^5	12	0.008	2.45
Cluster 143	2.30 x 10^5	100	0.0004	1.96
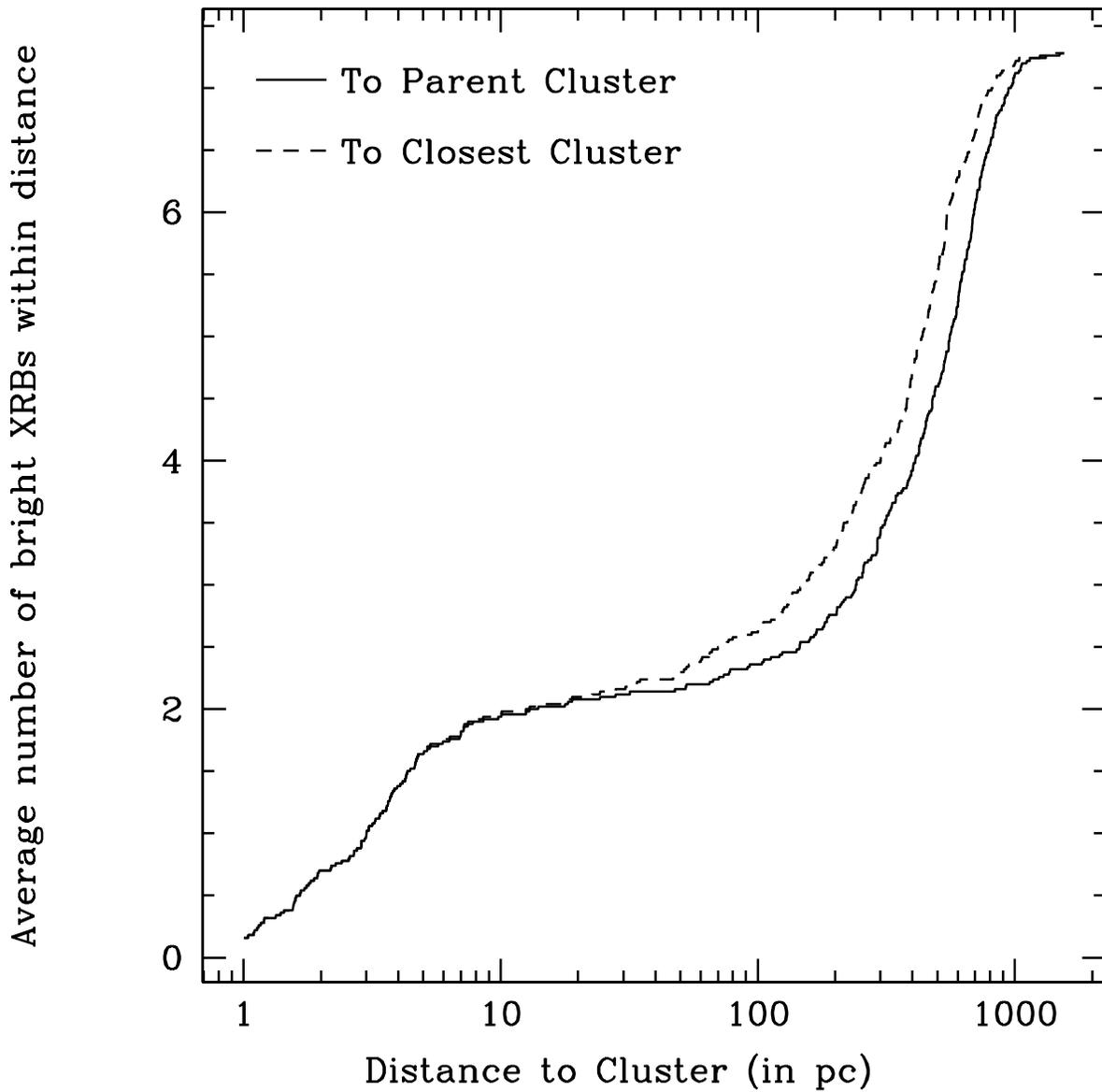
Fig. 1.— Average number of XRBs above a cutoff of $L_X = 1e36$ erg s^{-1} made in Cluster A per run within the given distance to Cluster A / nearest Cluster (including Cluster A)
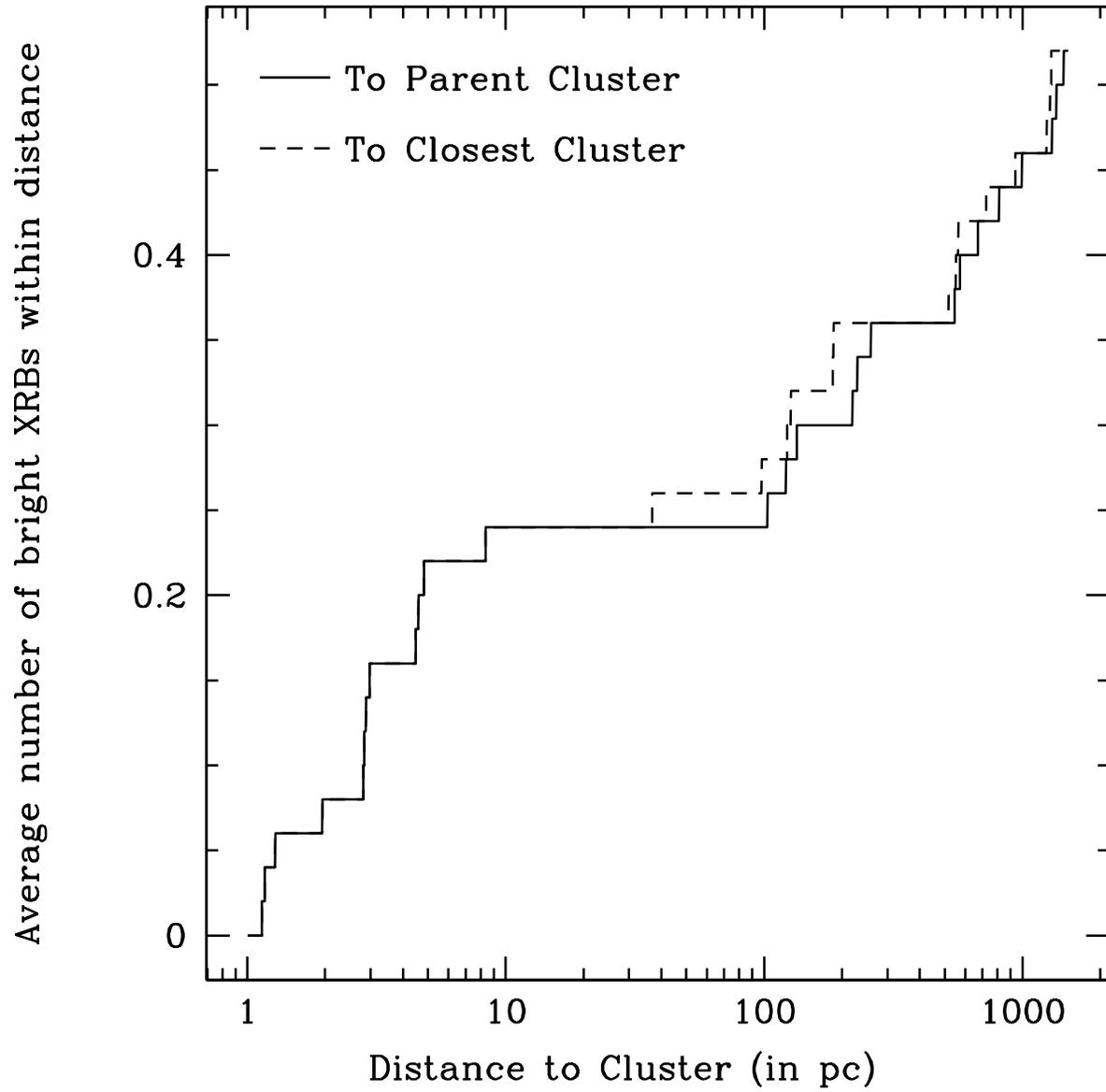
Fig. 2.— Same as Figure 1 for Cluster B
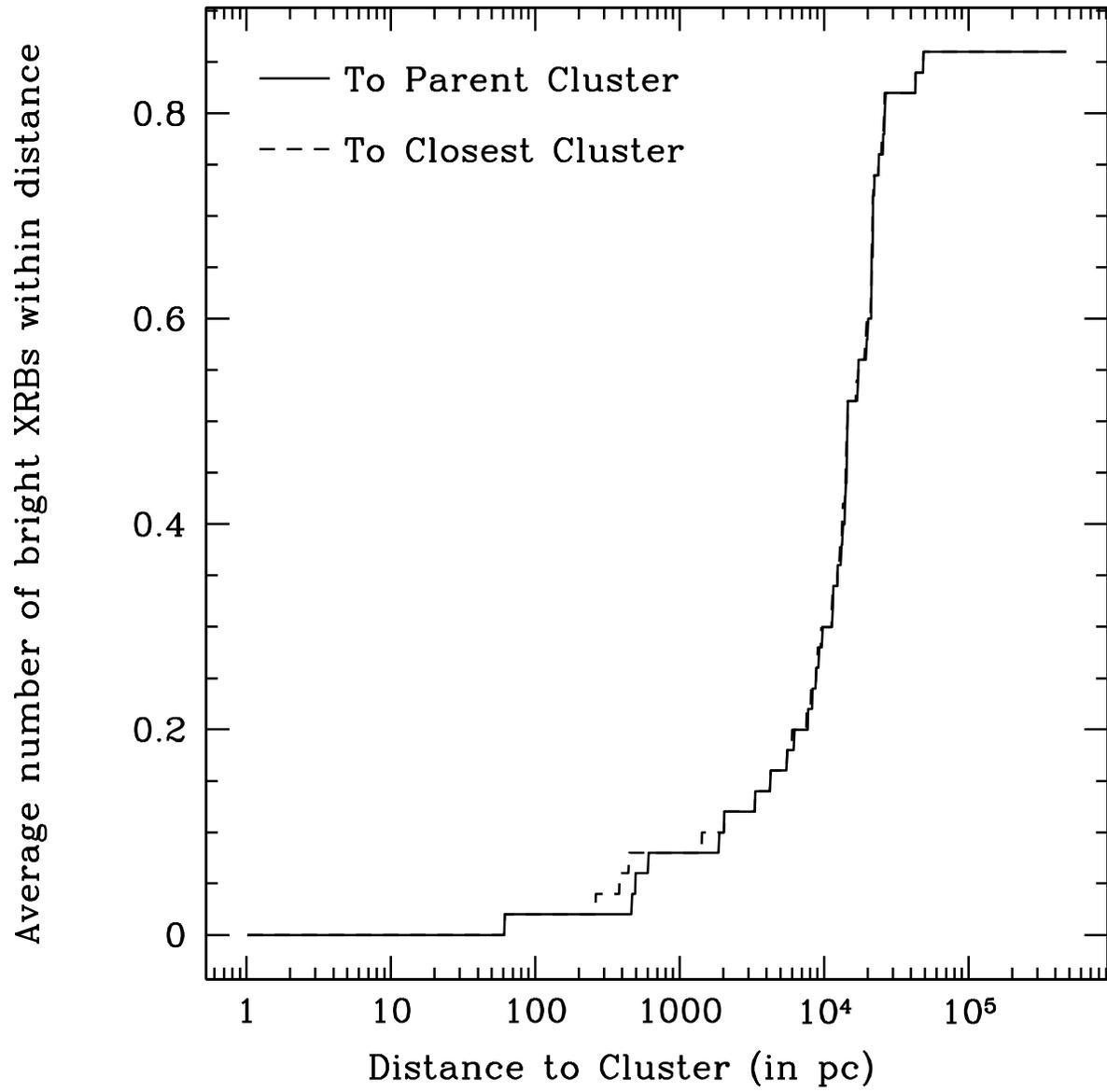
Fig. 3.— Same as Figure 1 for Cluster 143 (A04, Cluster 35 from Hunter et al. (2000))

22

dim XRBs, with luminosities $< 3 \times 10^{36}$ erg s^{-1}, and very distant (>100 pc), XRBs falling along a range of luminosities. We note the almost complete lack of intermediate luminosity systems near the cluster center.

We find that at an age of 12 Myr (the age we adopt for both Clusters A and B), there are two general pathways for bright system creation. Since we are using a very high luminosity cutoff of $L_X = 1e36$ erg s^{-1} we have a strong selection towards extremely bright mass transfer XRBs. Wind accretion systems are more important in the first 5-10 Myr of evolution, but by 12 Myr, most donor stars large enough to create the strong winds needed for bright accretion have undergone their own supernova events, leading to the creation of non X-Ray bright compact object binaries.

The exception to this rule are donors currently in the hydrogen rich, helium core burning phase. In this short lived state of stellar evolution, the donor star is burning helium, but still possesses a large hydrogen rich envelope. Due to the high temperature of helium burning, these systems have massive radii and are thus able to generate extremely strong winds. However, there are two constraints on these systems. First, they are still relatively dim, compared to the often Eddington limited mass transfer sources. Secondly, the systems must have a very wide orbit, because the binary must not form a common envelope when the donor star enters helium core burning. If a common envelope is established, it will quickly be lost, following the energy prescription of Webbink (1984), ending the wind accretion stage. Because of the necessity for wide orbits, the compact objects natal kick must be extremely small, as these systems are easily split. Thus Helium Core burning wind systems are almost entirely restricted to be both dim and very near their parent cluster.

In attempting to understand the differences between these systems, we note that the only large difference between Cluster A and B is the much lower metallicity of Cluster A. In terms of the number of XRBs produced, the only two relevant effects are the mass of the cluster, which has a linear effect on the number of bright systems, and the metallicity.
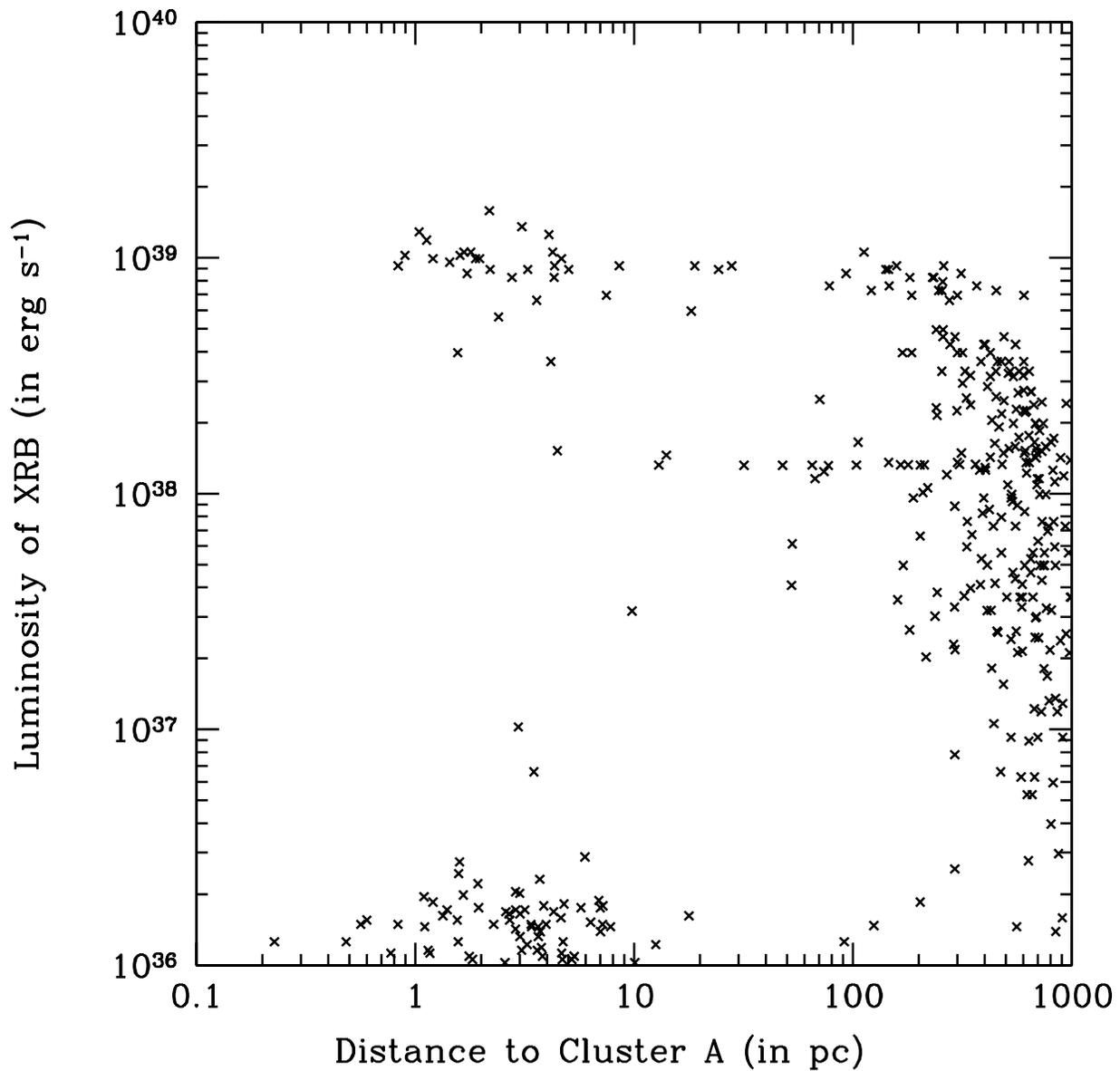
Fig. 4.— Distance from Cluster center versus luminosity for XRBs with a luminosity over the cutoff of $L_X = 1e36$ erg s^{-1} produced in Cluster A
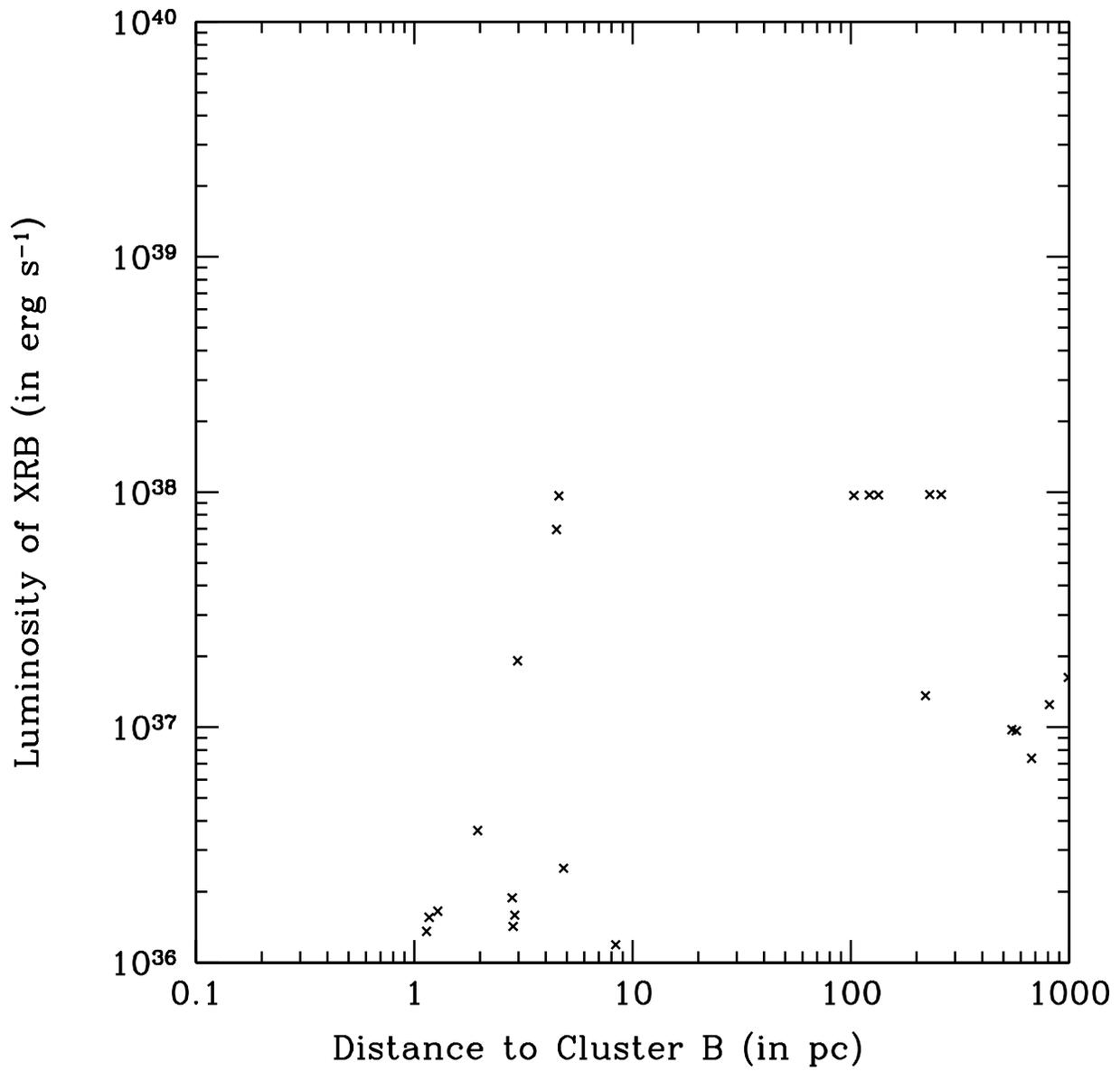
Fig. 5.— Same as Figure 4 for Cluster B
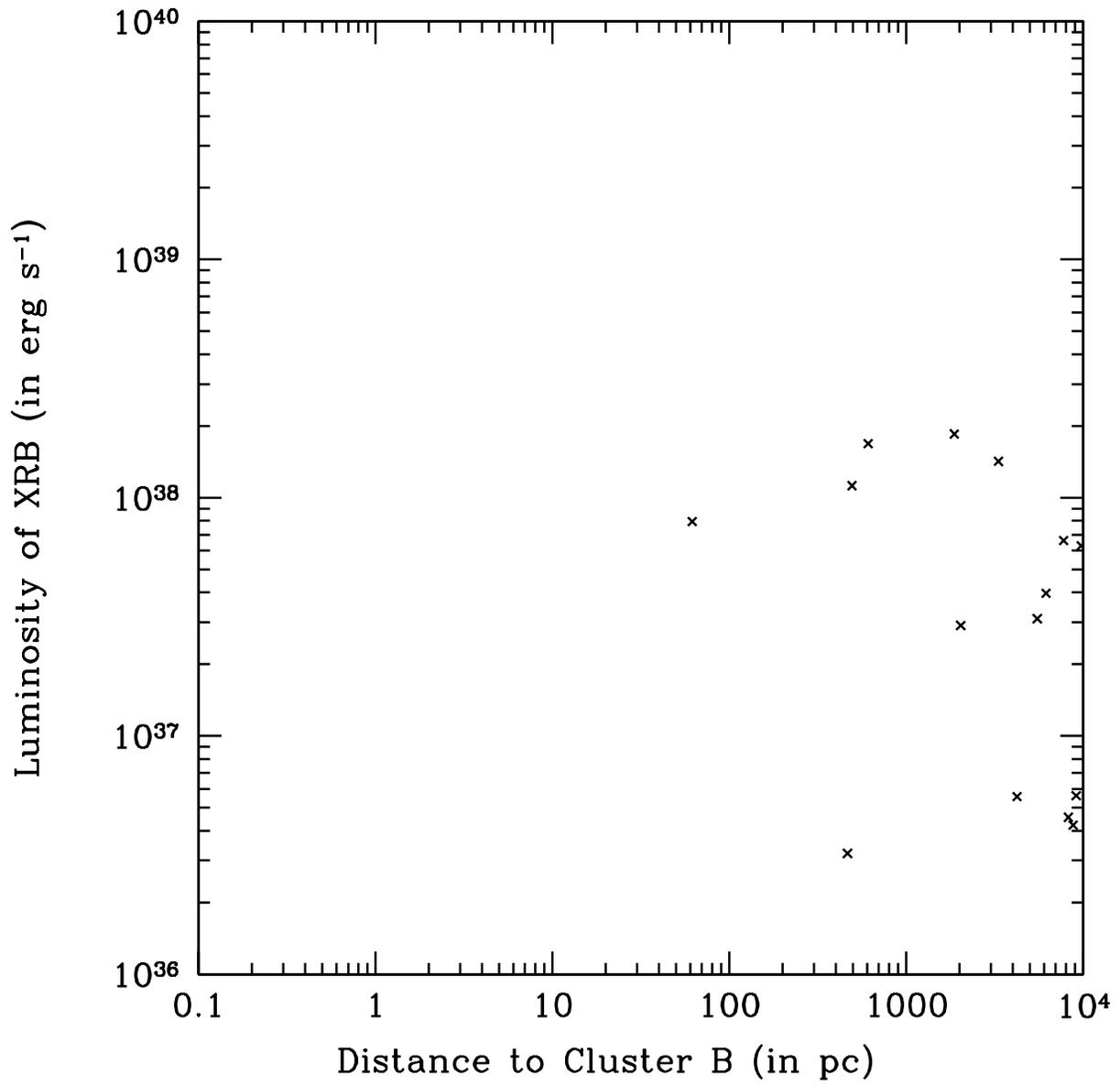
Fig. 6.— Same as Figure 4 for Cluster 143 (A04, Cluster 35 from Hunter et al. (2000))

Cluster A is approximately three times as massive as Cluster B, yet we note that Cluster A produces ∼12 times the number of bright XRBs as Cluster B. The additional factor of four preference for XRB formation in Cluster A is obviously connected to the preferential formation of XRBs in low metallicity clusters.

As shown in previous work (Linden 2008), there are several effects which lend themselves to greater XRB production from young starbursts at low metallicity. Most importantly, high metallicity XRBs are required to have a larger initial periastron separation in order to avoid dynamically unstable interactions during stellar evolution. In high metallicity systems, star photospheres absorb and re-emit much more energy, leading to a hotter photosphere and larger stellar radius. (Schaller et al. 1992; Hurley et al. 2000). Though high metallicity stars contain a larger stellar radius throughout their active lives, the effect is most important as the star transfers through the Hertzsprung Gap, the period between the end of the core hydrogen burning and the onset of core helium burning. During this stage, hydrogen in the shell around the core burns, and the stars radius expands significantly. However, there is no clear cut entropy boundary between the core and envelope at this stage (Ivanova & Taam 2004). Thus common envelope phases, where two binary partners share the same outer envelope, cannot simply cause the envelopes to be ejected, leaving the two stellar cores intact. Instead, a common envelope phase during either companions evolution through the Hertzsprung gap is thought to lead to dynamic instabilities and inspiral (Taam & Sandquist 2000; Belczynski et al. 2008).

For this work, we note that Hertzsprung Gap common envelopes are an important effect not only in determining the survivability of XRB progenitors in Clusters A and B, but also in creating the spatial distribution of sources created by the two clusters. Despite the fact that we create kick velocities with a Maxwellian distribution, the resulting kick distribution of observed XRBs is certainly not Maxwellian, because kicks of energy higher than the binding energy of the system will tend to break up the binary. Thus, there is a selection

effect towards low kick binaries, with the strength of the effect inversely related to the binding energy of the XRB progenitor. Since low metallicity binaries can survive in closer orbits, more high kick systems are allowed to survive. This is apparent in Figures 1 and 2 where ∼70% of Cluster A's XRBs have travelled more than 100 pc from the Cluster center while only ∼45% of Cluster B's XRBs have travelled this distance.

It is interesting to discover that due to the age of Cluster 143, it is likely any XRBs produced in this cluster are too distant to be observed, despite the fact that Cluster 143 actually produced the second most XRBs of all clusters in our simulation. Comparing the activity between Clusters A and 143, we note that the most important difference is the system age. Here our analysis agrees with that of S05. We find that for older clusters, systems are preferentially located much farther away from the cluster center, as they have had more time to travel. However, since each XRB only receives one kick (at the supernova event of the primary star), we would expect any system that does not become unbound to stay in the SSC potential well forever. Since we found XRBs in Cluster A which are clearly bound to the cluster, we would expect the same for Cluster 143. The only way to lose all bound systems would be if systems from this region of parameter space simply turn off by 100 Myr.

In order to understand this, we note the different types of systems which were bright at 12 Myr in Cluster A. Earlier, we described how the only wind accretion systems this bright have helium core burning donors. Even if we have a helium burning donor, we still need an extremely massive system in order to exceed the luminosity cutoff of $L_X = $ 1e36 erg s^{-1}, and these donors all undergo their own supernova events before 100 Myr. Subsequently, they are not important in the analysis of Cluster 143.

The other type of close system are mass transfer systems which received very small kicks. There are two ways for a binary system to gain a small natal kick velocity. Either the black hole must have undergone direct collapse, or the system must have a combination of a

"lucky" small kick, and a large donor star so that the total velocity imparted to the system is low. Both of these effects are ruled out at 100 Myr, because all the large donors have undergone their own supernova events. The bright mass transfer systems at this age all have very tightly bound systems which could survive large kicks, and thus all systems are very far away from the parent cluster. Since these systems have a low mass main sequence donor, they are very bright on all analyzed timescales, and form an expanding line of the most distant XRBs in all graphs.

5.1. Comparison with Kaaret et al. (2004)

We note several key points of agreement with Martin et al. (2002) and K04. First, we have successfully matched the number of XRBs found in the galaxy, with our average runs producing ~ 11 sources, compared to the 12 observed sources in NGC 1569. Since there is both a large statistical variability in the number of bright sources we expect, as well as the ability to adjust many $StarTrack$ input parameters in order to shift the number of systems, we find it promising that we were able to obtain such a close match with our default inputs. Secondly, our results in Figure 4 show that while there are many sources far away from the cluster, the several brightest sources lie closest to Cluster A.

We find several inconsistencies with the observational data of K04. First, while K04 assigns a distance of 10 pc to all XRBs found within 10 pc of a cluster center (due to deviations in the measurement of the dynamic center of the SSC), they find relatively few sources inside this range, while we note a significant percentage of our XRBs stay very close to the cluster center. Instead, K04 finds many clusters between 10-100 pc away, while we see extremely few sources in this region. Secondly, we find several sources above a luminosity of 10^{38} erg s^{-1} at a distance between 100-1000 pc, while K04 does not see these sources.

There is one phenomena omitted from our analysis which nicely explains the first

discrepancy. K04 notes that another method of moving binaries outside of SSCs is through dynamic interactions between binary systems. There have been numerous studies into the impact of these N-body interactions. Portegies Zwart et al. (1999) showed that dynamic interactions in very dense star clusters could cause the ejection of binary systems on timescales of several Myr. Joshi et al. (2001) used Monte Carlo methods to calculate this effect and show that the ejection velocities depend on the velocity dispersion of the cluster. We note this implies that escaping XRBs will have velocities just over the escape velocity of the cluster, and thus will move only short distances from the cluster on timescales in which most XRB are luminous. While direct calculation of this effect would require a full N-body simulation of the SSC which is outside the scope of this work, we note that inclusion of the dispersion effect could only improve our models with respect to K04 observation by moving our systems from 0-10 pc to 10-50 pc, eliminating our overabundance of low distance systems to fill the gap of medium distance systems.

The second discrepancy is more difficult to explain. First we note we only see these extremely bright, distant XRBs in Cluster A, while no distant XRBs over the K04 cutoff of 1×10^{38} erg s^{-1} are observed in our other runs. We note that the existence of these systems depends either on a "lucky" kick both with a high velocity and in a direction such that it does not destroy the system, or on the system establishing a very tight orbit prior to the first supernova event, such that it can survive an extremely energetic kick and remain tightly bound. By individually checking the bright systems which were propelled far away from the cluster center, we find the latter explanation to be true. Due to the many free variables in population synthesis code, alterations in any one of several variables could solve the disagreement. There is one obvious candidate for eliminating these systems. We note that the A04 observation of Cluster A's metallicity as z=0.0004 is unusually low, and that Hunter et al. (2000) instead found a metallicity of z=0.004. If we increase our cluster metallicity, we cause Hertzsprung gap common envelopes to restrict the formation of these

extremely tight binary systems. Testing a run of Cluster 7 at this higher metallicity, we found the brightest distant systems to be entirely eliminated. However, this also decreased the number of XRBs formed in Cluster A by a factor of 3, which hurts our correlation with the overall number of bright XRBs in the galaxy. Further research is warranted into the parameter space which affects this class of bright and distant systems.

6. Future Research

Our immediate goal is to explore the expanded parameter space of XRB production in order to obtain a better match with NGC 1569. However, we have currently been sidetracked with a more promising project involving an attempt to model XRB formation in the Small Magellanic Cloud (SMC), which is a nearby dwarf galaxy which underwent a burst of star formation activity approximately 30-60 Myr ago in a 0.5x2.0 pc^2 region referred to as "the bar" (Maragoudaki et al. 2001; Harris & Zaritsky 2004; Bekki & Chiba 2005) The SMC has been found to contain a large population of low velocity wind accretion XRBs with eccentric B star donors (Be-XRBs) (Coe 2005). One of the most difficult problems in previous attempts to model the SMC was in obtaining the necessary $\sim$50 Be-XRB sources without obtaining a large population of bright mass transfer XRBs which are not observed in the starburst region of the SMC (J. Gallagher, A. Zezas, 2008, private communication).

Our results point towards a unique explanation for the lack of mass transfer black holes observed in the SMC. At all but the youngest ages, almost all very bright systems are found very far from the region in which they were formed. Our results show that at 30 Myr, all direct collapse black holes and helium core burning wind accretion systems have already disappeared. Thus the expected mass transfer background may be entirely dispersed outside of the bar region. While we have not discussed the creation of Be-XRBs in this work (as our code construes them to lie below the 1e36 erg s^{-1} cutoff used for our

NGC 1569 modeling) we do have new insights for a method of explaning these systems (Linden 2008). However, even given the creation of many Be-XRB systems, a discussion showing the rapid disappearance of bright MT sources will be critical for explaining SMC observations. As there have been many previous unsuccessful attempts at modeling the SMC, this finding presents a particularly exciting avenue for research.

7. Discussion and Conclusions

In order to model observational evidence showing that XRBs are preferentially found nearby SSCs, we vastly modified the *StarChart* evolution code (S05). In order to allow the modeling of a starburst galaxy, we allowed for restricted three body motion of the cluster-XRB-galaxy system, and we created galactic potentials following the Plummer-Kuzmin model. We also fixed several important problems such as the interpolation of *StarTrack* XRB luminosities, and improved the code's adaptability to desired user input.

Using this improved code, we successfully modeled the starburst galaxy NGC 1569, and explained the dominant methods of XRB formation which are important in the galaxy. We showed that XRB formation is likely dominated by Cluster A, due to its extremely low metallicity. We also showed that our results are reasonably consistent with observation, if we allow for our bound XRBs to become slightly unbound due to dynamic interactions. We believe our current results will form an important component of explaining the long-standing puzzle of XRB formation in the SMC.

8. Acknowledgments

REFERENCES

Aarseth, S. J., Henon, M., & Wielen, R. 1974, A&A, 37, 183

Anders, P., de Grijs, R., Fritze-v. Alvensleben, U., & Bissantz, N. 2004, MNRAS, 347, 17

Arp, H., & Sandage, A. 1985, AJ, 90, 1163

Barnes, J. E., & Hernquist, L. E. 1991, ApJ, 370, L65

Bekki, K., & Chiba, M. 2005, MNRAS, 356, 680

Belczynski, K., Kalogera, V., Rasio, F. A., Taam, R. E., Zezas, A., Bulik, T., Maccarone, T. J., & Ivanova, N. 2005, ArXiv Astrophysics e-prints

—. 2008, ApJS, 174, 223

Coe, M. J. 2005, MNRAS, 358, 1379

Cordes, J. M., & Chernoff, D. F. 1998, ApJ, 505, 315

de Grijs, R., Gilmore, G. F., Johnson, R. A., & Mackey, A. D. 2002, MNRAS, 331, 245

de Marchi, G., Clampin, M., Greggio, L., Leitherer, C., Nota, A., & Tosi, M. 1997, ApJ, 479, L27+

Fabbiano, G. 1989, ARA&A, 27, 87

Fryer, C. L., & Kalogera, V. 2001, ApJ, 554, 548

Gonzalez Delgado, R. M., Leitherer, C., Heckman, T., & Cerviño, M. 1997, ApJ, 483, 705

Gonzalez-Delgado, R. M., Perez, E., Diaz, A. I., Garcia-Vargas, M. L., Terlevich, E., & Vilchez, J. M. 1995, ApJ, 439, 604

Grimm, H.-J., Gilfanov, M., & Sunyaev, R. 2003, MNRAS, 339, 793

Gunn, J. E., & Ostriker, J. P. 1970, ApJ, 160, 979

Harris, J., & Zaritsky, D. 2004, AJ, 127, 1531

Ho, L. C., & Filippenko, A. V. 1996, ApJ, 466, L83+

Hobbs, G., Lorimer, D. R., Lyne, A. G., & Kramer, M. 2005, MNRAS, 360, 974

Hunter, D. A., Gallagher, J. S., & Rautenkranz, D. 1982, ApJS, 49, 53

Hunter, D. A., O'Connell, R. W., Gallagher, J. S., & Smecker-Hane, T. A. 2000, AJ, 120, 2383

Hurley, J. R., Pols, O. R., & Tout, C. A. 2000, MNRAS, 315, 543

Israel, F. P. 1988, A&A, 194, 24

Israel, F. P., & de Bruyn, A. G. 1988, A&A, 198, 109

Ivanova, N., & Taam, R. E. 2004, ApJ, 601, 1058

Joshi, K. J., Nave, C. P., & Rasio, F. A. 2001, ApJ, 550, 691

Kaaret, P., Alonso-Herrero, A., Gallagher, J. S., Fabbiano, G., Zezas, A., & Rieke, M. J. 2004, MNRAS, 348, L28

Linden, T. 2008, Undergraduate Senior Physics Thesis, Northwestern University, 1, 1

Makishima, K., Kubota, A., Mizuno, T., Ohnishi, T., Tashiro, M., Aruga, Y., Asai, K., Dotani, T., Mitsuda, K., Ueda, Y., Uno, S., Yamaoka, K., Ebisawa, K., Kohmura, Y., & Okada, K. 2000, ApJ, 535, 632

Maragoudaki, F., Kontizas, M., Morgan, D. H., Kontizas, E., Dapergolas, A., & Livanou, E. 2001, A&A, 379, 864

Martin, C. L., Kobulnicky, H. A., & Heckman, T. M. 2002, ApJ, 574, 663

Miyamoto, M., & Nagai, R. 1975, PASJ, 27, 533

Plummer, H. C. 1911, MNRAS, 71, 460

Portegies Zwart, S. F., Makino, J., McMillan, S. L. W., & Hut, P. 1999, A&A, 348, 117

Reakes, M. 1980, MNRAS, 192, 297

Recchi, S., Hensler, G., Angeretti, L., & Matteucci, F. 2006, A&A, 445, 875

Recchi, S., Matteucci, F., & D'Ercole, A. 2001, MNRAS, 322, 800

Schaller, G., Schaerer, D., Meynet, G., & Maeder, A. 1992, A&AS, 96, 269

Sepinsky, J., Kalogera, V., & Belczynski, K. 2005, ApJ, 621, L37

Stil, J. M., & Israel, F. P. 1998, A&A, 337, 64

Taam, R. E., & Sandquist, E. L. 2000, ARA&A, 38, 113

Waller, W. H. 1991, ApJ, 370, 144

Webbink, R. F. 1984, ApJ, 277, 355